Transactions, SMiRT-23
Manchester, United Kingdom - August 10-14, 2015
Division IV, Paper ID 401

Tsunami Hazard in the Arabian Gulf Due to Earthquakes in the Makran Subduction Zone

Jeffrey A. Oskamp[1], Ahmed "Jemie" A. Dababneh[2], and Daniel J. Barton[3]

[1] Engineering Associate, RIZZO Associates, USA
[2] Managing Principal, RIZZO Associates, USA
[3] Vice President, RIZZO Associates, USA

ABSTRACT

A tsunami analysis was conducted to quantify the tsunami hazard in the western Arabian Sea and inside the Arabian Gulf due to seismic activity in the Makran Subduction Zone (MSZ). The MSZ extends across the Arabian Sea from east to west. It is the closest subduction zone fault to the Arabian Gulf and considered the main source of tsunami activity affecting the western Arabian Sea and the Arabian Gulf.

The analysis conservatively postulates a rupture along the entire length of the MSZ. The resulting earthquake could have a moment magnitude (M_w) of approximately 9.0, which is significantly larger than the largest earthquake recorded in this region. The associated sea floor displacement is computed based on the methodology of Okada (1985).

A hydrodynamic model is developed using Delft3D-FLOW to simulate the initiation and propagation of the tsunami wave. The study indicates significant tsunami hazards on the shores of the Arabian Sea, but that minimal tsunami energy enters the Arabian Gulf through the Strait of Hormuz.

INTRODUCTION

Tsunami hazards are important design considerations for any coastal structure. The hydrodynamic forces that a tsunami wave exerts on an inundated structure require meticulous attention in design if a structure is to be built in a potential tsunami inundation area. Alternately, knowledge of potential tsunami inundation areas can affect planning to ensure that vital structures are built at high enough elevations and away from tsunami-prone areas.

Some stretches of coastline are well known for their tsunami hazards (e.g., Japan). Other areas may have more infrequent tsunami events or events of smaller magnitudes. The frequency and severity of tsunamis along a particular coastline are a function of the proximity and characteristics of potential tsunami generating mechanisms. Tsunami waves can be generated by seismic activity, volcanic activity, submarine landslides, and potentially other mechanisms (including combinations of the events listed above).

This study considers the potential for co-seismically generated tsunami waves from the Makran Subduction Zone (MSZ) to affect the coastlines in the western Arabian Sea and the coasts inside the Arabian Gulf. The MSZ (Figure 1) is the nearest subduction zone to the Arabian Gulf. A conservative tsunami scenario was developed for the purposes of this study. The tsunami generation and propagation were simulated using a tsunami propagation model that was verified and calibrated by simulating the historic 1945 tsunami that originated in the MSZ.

MAKRAN SUBDUCTION ZONE GEOMETRY

The MSZ is located along the southern coasts of Pakistan and Iran (Figure 1). The MSZ extends from the Strait of Hormuz to near Karachi, Pakistan. Byrne et al. (1992) provides a good discussion of the MSZ geometry. The MSZ corresponds to a portion of the boundary between the Eurasian Plate (to the

north) and the Arabian Plate (to the south). The length of the MSZ is approximately 900 to 1000 kilometres (km).

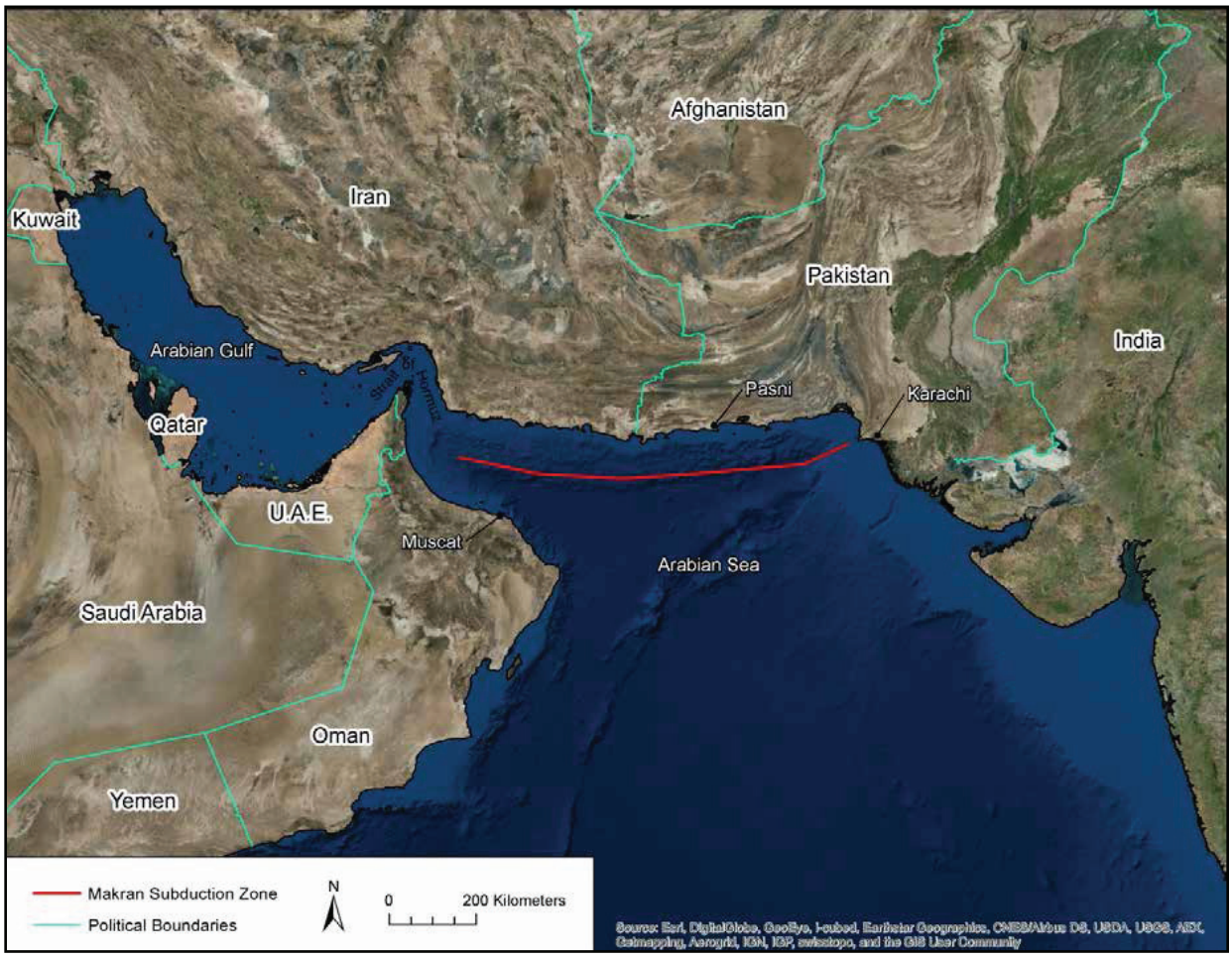

Figure 1: Location of Makran Subduction Zone – Study Area

The largest recorded earthquake in the MSZ is the November 1945 earthquake, with a moment magnitude (M_w) of 8.1. The great 1945 earthquake generated a large tsunami wave which impacted the nearby cities of Pasni and Ormara, Pakistan (Byrne et al., 1992). The tsunami was also felt at more distant locations such as Karachi, Pakistan and Muscat, Oman. Some information is also available from historic earthquakes that were not recorded with modern technology (Bilham et al., 2007).

The geometry of the MSZ is summarized in Byrne et al. (1992), which indicates a strong segmentation between the east and west portions of the MSZ (in terms of seismicity). The plate boundary in eastern Makran has experienced great thrust earthquakes in the past and shows current moderate levels of seismicity. In contrast, no well-documented great earthquakes exist in the historic record for western Makran.

RUPTURE PARAMETERS AND SEA FLOOR DEFORMATION

Based on the segmented nature of the MSZ and the low seismicity of the western Makran (described above), it is considered unlikely (and thus very conservative) that single mega-thrust rupture would occur along the entire length of the MSZ. However, for the purposes of this analysis, such a

conservative scenario is postulated. This study considers the potential effects of a rupture along the entire length of the MSZ. This rupture would have a length of approximately 900 to 1000 km (1000 km to be conservative).

The moment magnitude that could be associated with such a full length rupture of the MSZ was estimated from the empirical relationship of Strasser et al. (2010), which indicates that for a fault length of 1000 km, the moment magnitude would be approximately M_w 9.0.

Other fault parameters such as fault width, dip angle, and rake angle, were developed based on references such as Strasser et al. (2010), Ward (1989), Synolakis et al. (1997), and Byrne et al. (1992). Fault parameters were developed both for the M_w 9.0 earthquake representing a full rupture along the length of the MSZ and for the historic 1945 earthquake for calibration purposes.

Based on the fault geometries developed, the sea floor displacements were estimated using the method of Okada (1985). The sea floor displacement profiles are illustrated in Figures 2 and 3 for the historic 1945 earthquake and the hypothetical M_w 9.0 earthquake, respectively (contours represent vertical displacements in meters).

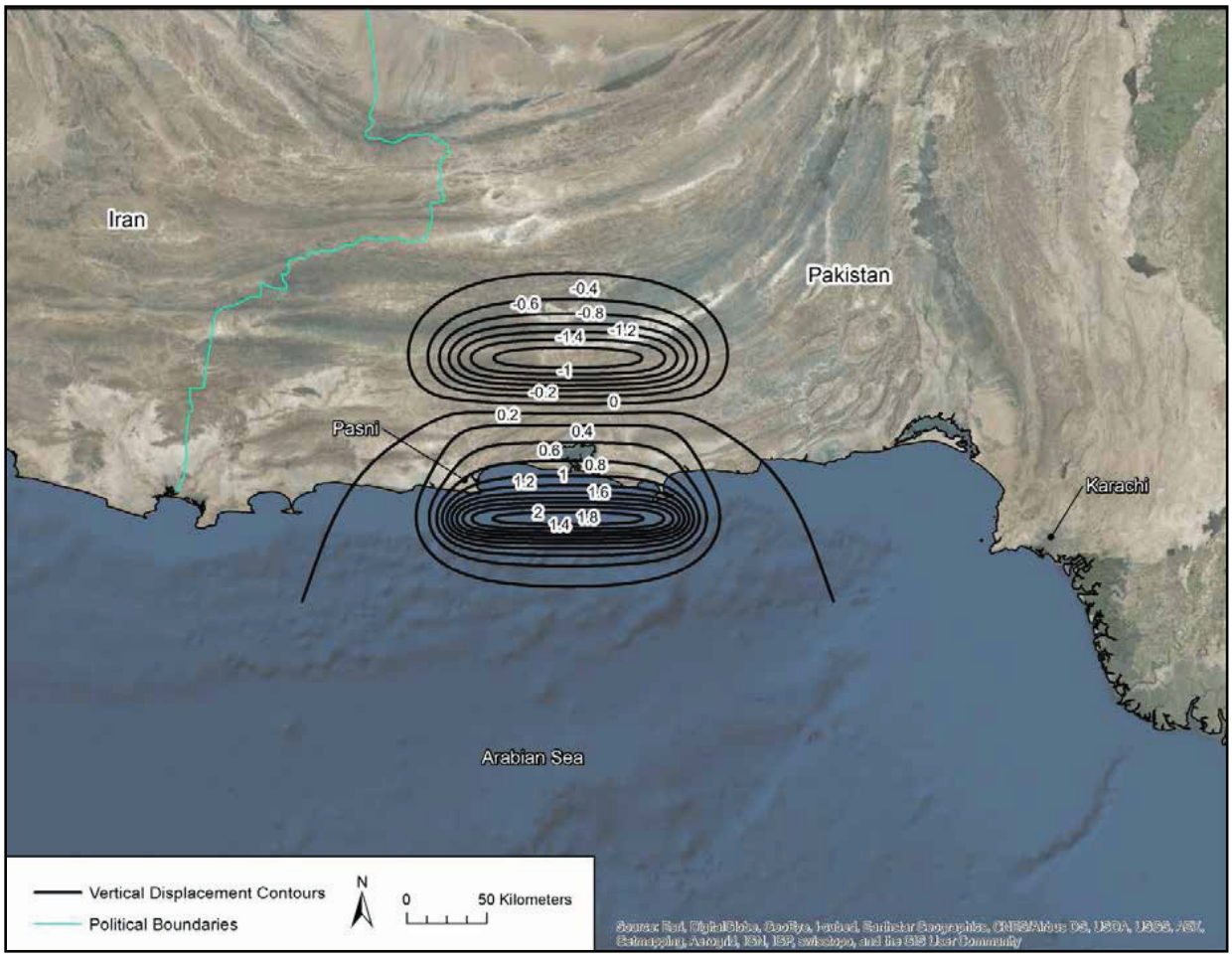

Figure 2: Sea Floor Displacement for 1945 Earthquake

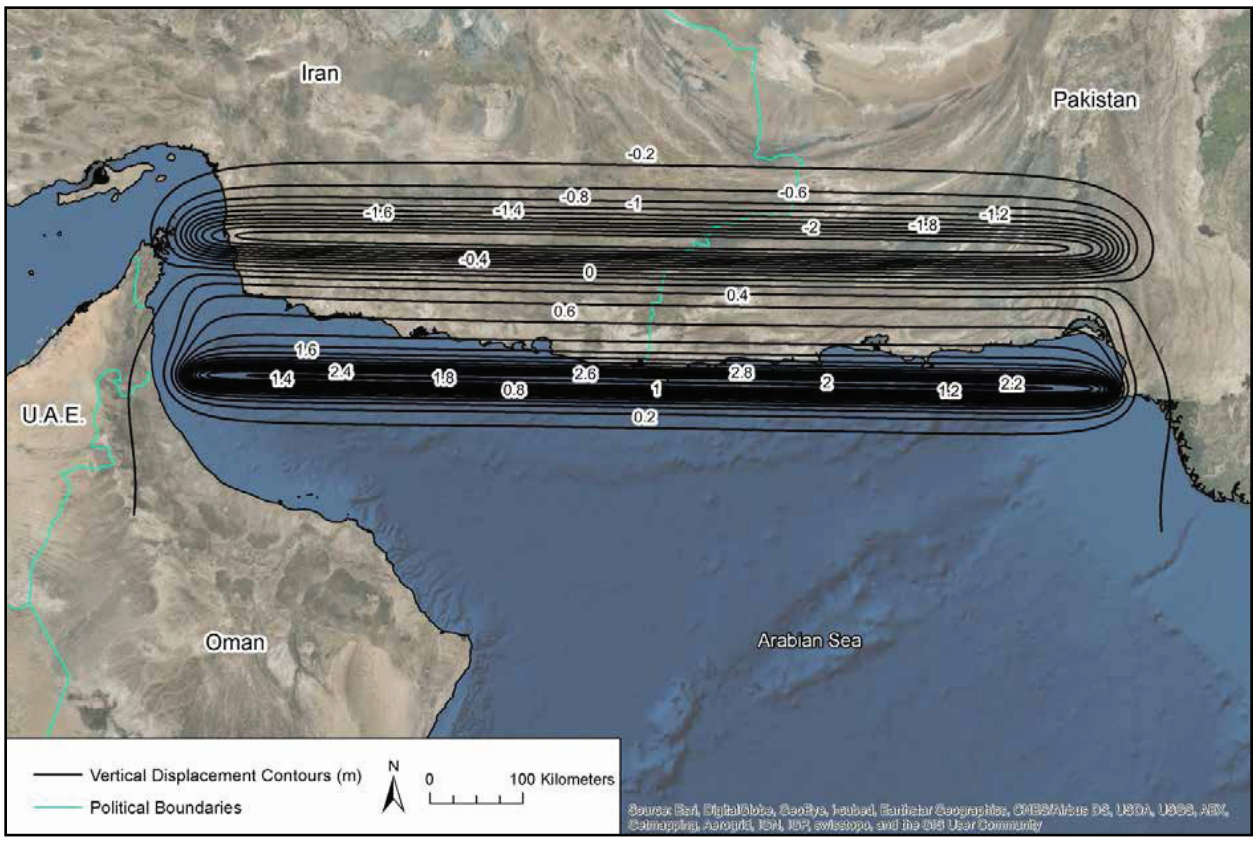

Figure 3: Sea Floor Displacement for Hypothetical M_w 9.0 Earthquake

HYDRODYNAMIC MODEL FORMULATION, VALIDATION, AND CALIBRATION

A model was developed in Delft3D-FLOW (Deltares, 2011) to simulate tsunami propagation. The model domain (Figure 4) covers the northern portion of the Arabian Sea, as well as the entire Arabian Gulf. As appropriate for a moderately large domain, the model is constructed in spherical coordinates (to avoid distortions caused by rectangular projections). The grid resolution for the overall tsunami model was defined as one arc minute in both latitude and longitude (in linear units along the earth surface, this corresponds to approximately 1.8 km or less, but varies slightly throughout the domain). This resolution is finer than that used for some other tsunami models of this region (e.g., Heidarzadeh et al., 2009).

Parameter specifications for various other model parameters (e.g., bottom roughness coefficients, eddy viscosity, timestep, etc.) were made in accordance with the Delft3D-FLOW user manual (Deltares, 2011) and various literature sources (not discussed in detail in this paper).

For validation purposes, an even finer grid resolution of 12 arc seconds was applied for the shoreline near Pasni, Pakistan. The tsunami model was validated by comparing the tsunami results from the historic 1945 tsunami (generated by the sea floor displacement developed above [Figure 2]) to published records of the observed effects. In particular, the validation was performed by comparing the wave height observed at Pasni, Pakistan and the timing of the tsunami wave approaching Muscat, Oman.

There is some uncertainty as to the historic records of the tsunami effect at Pasni. Some records indicate that the largest tsunami wave occurred approximately 3.25 hours after the main shock of the earthquake, while other sources indicate shorter lag times of approximately 90 minutes to 120 minutes (Bilham et al., 2007). Some sources estimate a wave height of 12 to 15 meters at Pasni, while other sources indicate a more moderate (though still extreme) wave height of approximately 4 to 5 meters at Pasni (Heidarzadeh et al., 2008). Some literature has suggested that volcanic and/or landslide effects were

a significant factor in the 1945 Makran tsunami (e.g., Bilham et al. [2007] and Rajendran et al. [2008]). Particularly, these alternate processes could help explain the time lag between multiple tsunami waves reaching Pasni and/or the reports of larger (e.g., 12 to 15 meter) waves, if the reports are in fact true. The estimates of 4 to 5 meters are thought to be reliable and representative of the co-seismic tsunami effects of the 1945 event (Heidarzadeh et al., 2009). Consequently, the wave height of 4-5 meters near Pasni is used as the verification / calibration benchmark for this study.

Historical accounts also indicate that the tsunami wave reached Muscat, Oman approximately 45 minutes after the main earthquake (Rejenderan et al., 2008). This timing was verified in addition to the tsunami wave height at Pasni.

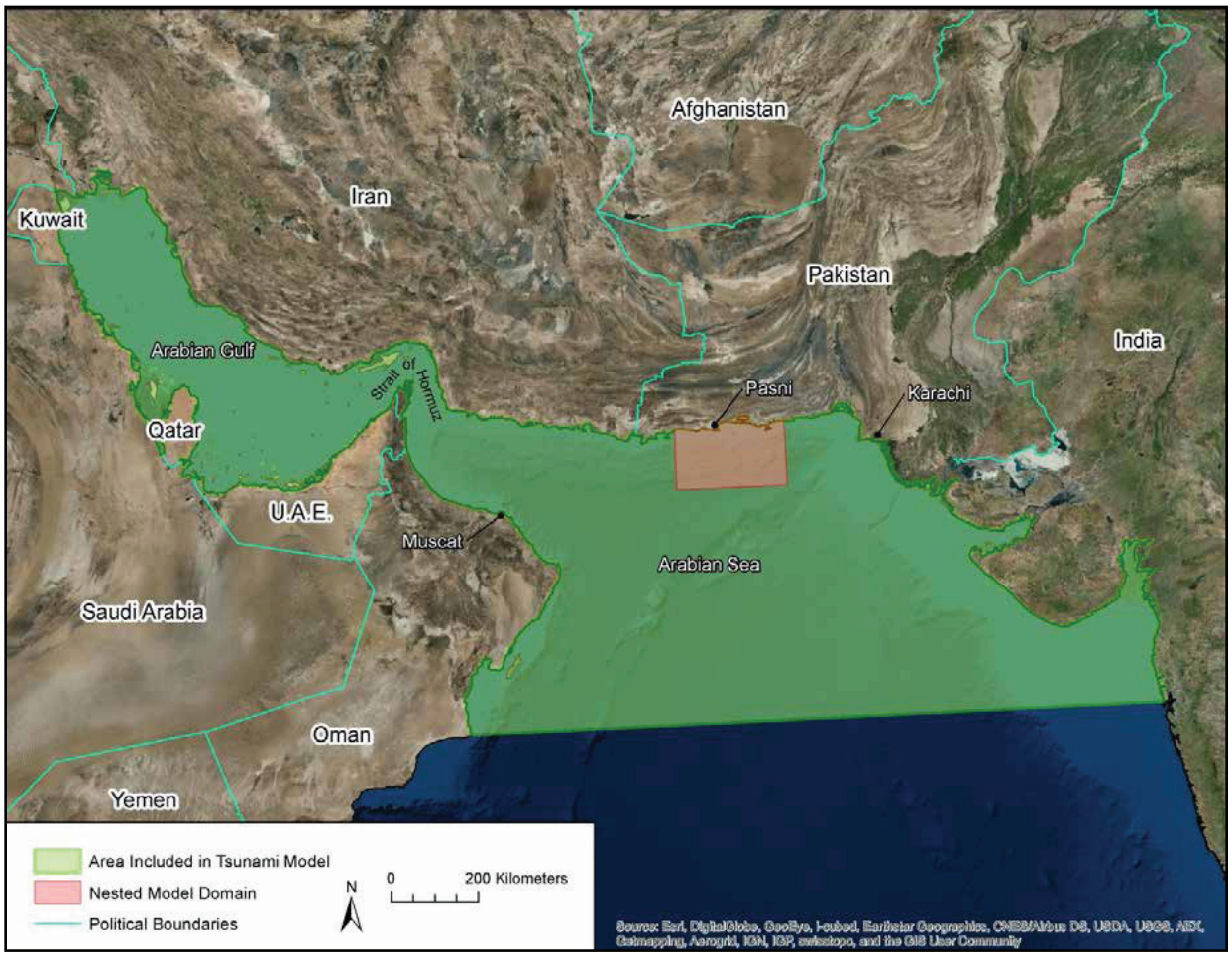

Figure 4: Tsunami Model Domains

Initial simulations for the 1945 tsunami (using the sea floor displacement shown in Figure 2) produced lower than expected tsunami wave heights at Pasni (approximately 3 meters). Since the positioning of the sea floor displacement effects of 1945 earthquake are not known precisely, the precise position of the sea floor displacement was considered a calibration parameter, governed by the various literature sources that suggest locations for the event. The calibrated location for the 1945 earthquake is visible with the results shown in Figure 5. The calibrated model produced a tsunami wave approximately 4.5 meters high at Pasni, which provides a reasonable comparison to the historic record, indicating that the model is operating appropriately. Figure 5 illustrates the peak tsunami wave amplitude at each point in

the model domain (i.e., not the water levels at a specific point in time). The variability in the wave amplitudes near the shoreline is indicative of the underlying bathymetric features.

The model indicated that the tsunami wave reached Muscat, Oman 49 minutes after the earthquake, which is reasonably comparable to the 45 minutes reported by Rejenderan et al. (2008). The calibration process indicated that the model developed for this analysis is operating appropriately for characterizing co-seismic tsunamis (tsunamis generated by sea floor displacements directly due to seismic ground motion).

It is important to note at this point that other mechanisms (e.g., submarine volcanos or submarine landslides) can be induced by an earthquake and lead to indirect tsunami generation. These effects are not accounted for in the tsunami model for this analysis. Some literature has suggested that volcanic and/or landslide effects were a significant factor in the 1945 Makran tsunami (e.g., Bilham et al. [2007] and Rajendran et al. [2008]). Particularly, these alternate processes could help explain the time lag between multiple tsunami waves reaching Pasni and/or the reports of larger (e.g., 12 to 15 meter) waves, if the reports are in fact true.

Since the effects of volcanoes and/or landslides are not included in the modelling or calibration process, any volcanic or landslide effects associated with the larger earthquake (evaluated below) are not evaluated.

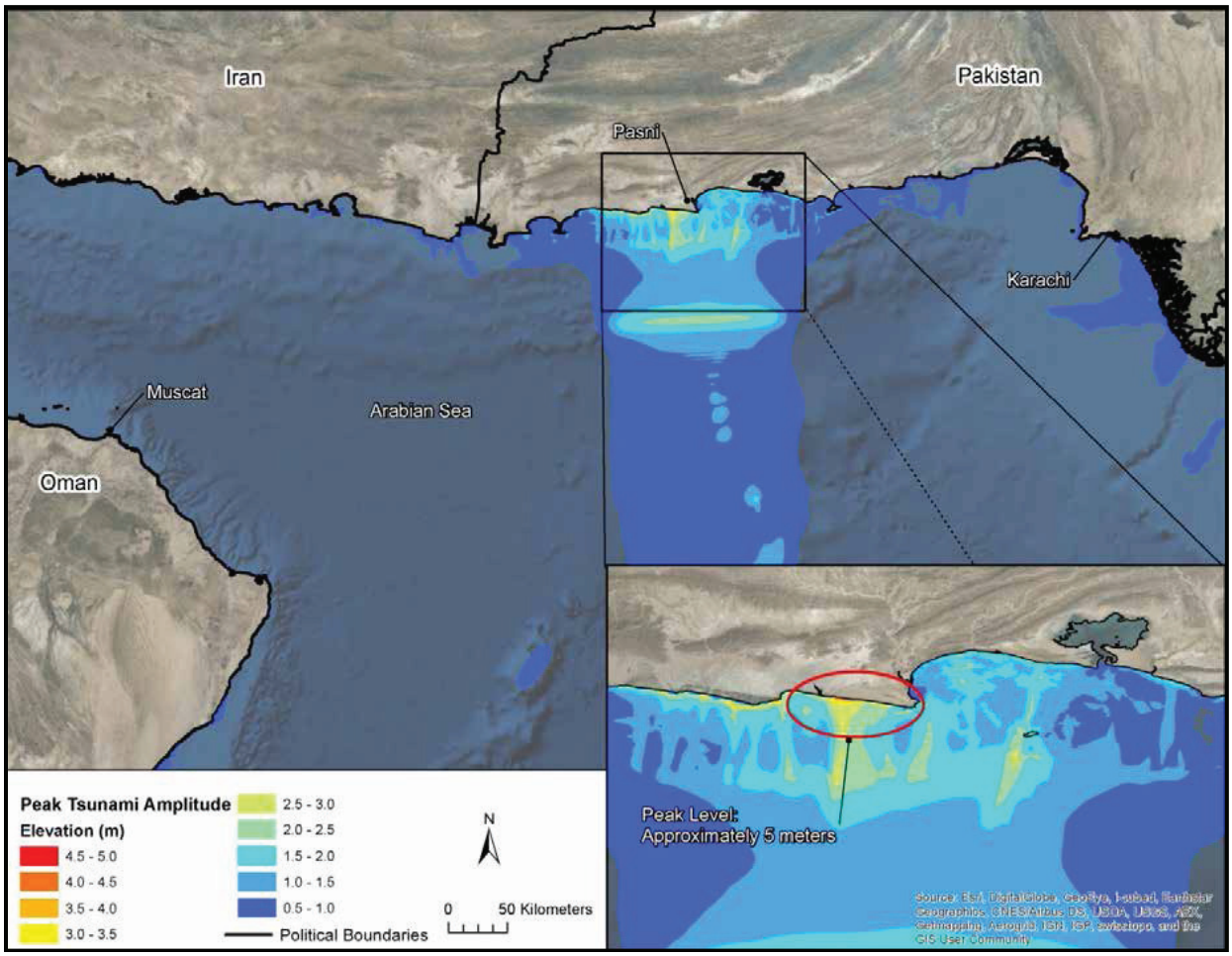

Figure 5: Calibration Simulation Results

RESULTS

After completing the model calibration, the M_w 9.0 tsunami was simulated. The peak tsunami wave amplitudes for the M_w 9.0 tsunami simulation are shown in Figure 6. This event causes large tsunami wave amplitudes (up to about 6 meters in some areas) along the southern coasts of Pakistan and Iran and the northern coast of Oman (Figure 7). The tsunami propagation model was simulated long enough to ensure that there were no remaining trapped wave energy that would amplify to create additional large tsunami waves.

Detailed results for the Arabian Gulf are illustrated in Figure 8. These results indicate that minimal tsunami energy propagates through the Strait of Hormuz. Peak tsunami amplitudes in the Strait of Hormuz are generally between 0.5 to 1.5 meters, but the tsunami wave spreads out as it enters the Gulf. Most of the Gulf coastlines are characterized by peak tsunami amplitudes of 0.3 meters or less, with higher amplitudes of up to 0.5 meters in some areas. These results are broadly consistent with the findings of Okal and Synolakis (2008), which also show that minimal tsunami energy enters the Arabian Gulf due to seismic activity in the MSZ.

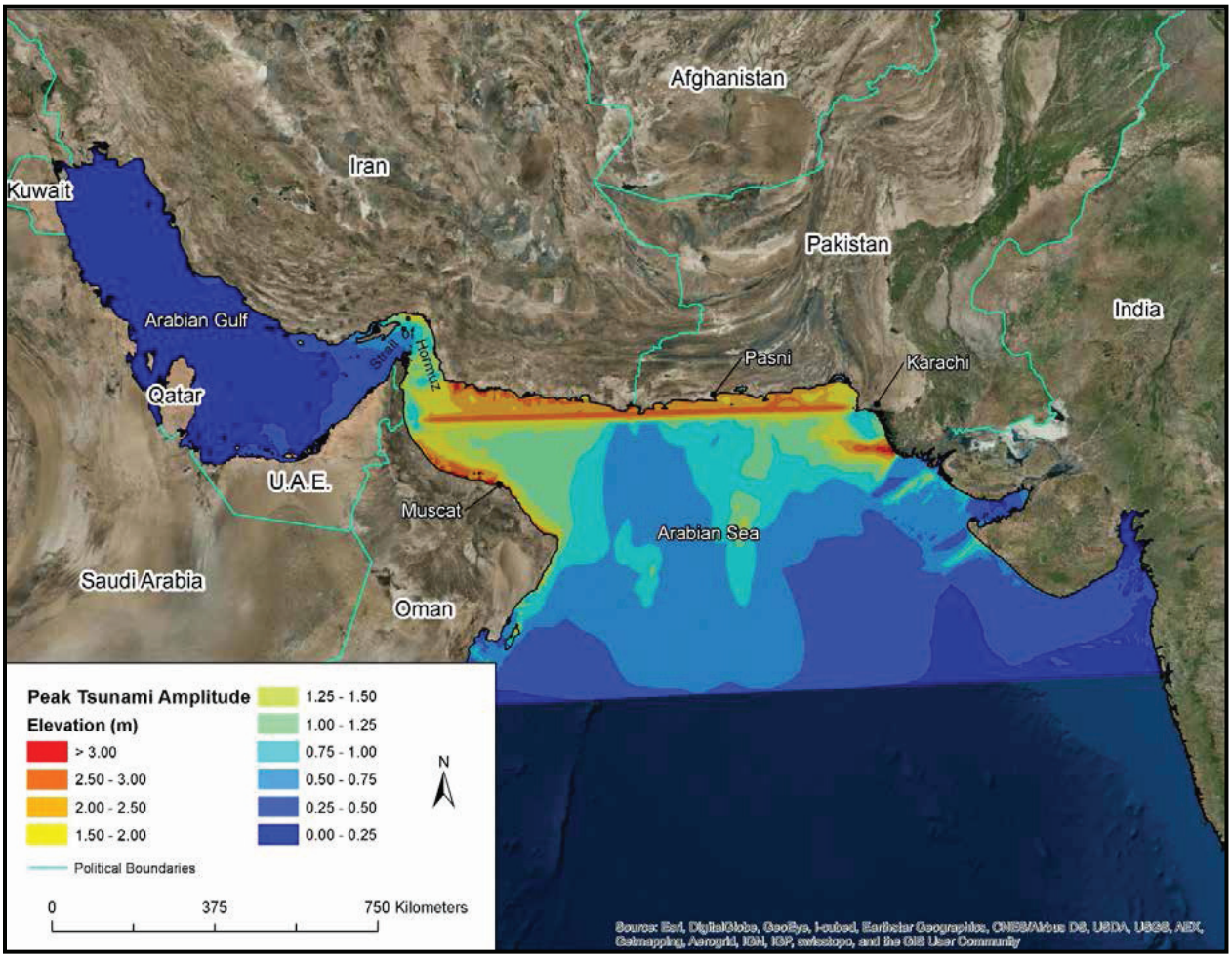

Figure 6: Peak Tsunami Wave Amplitudes for M_w 9.0 Earthquake Event

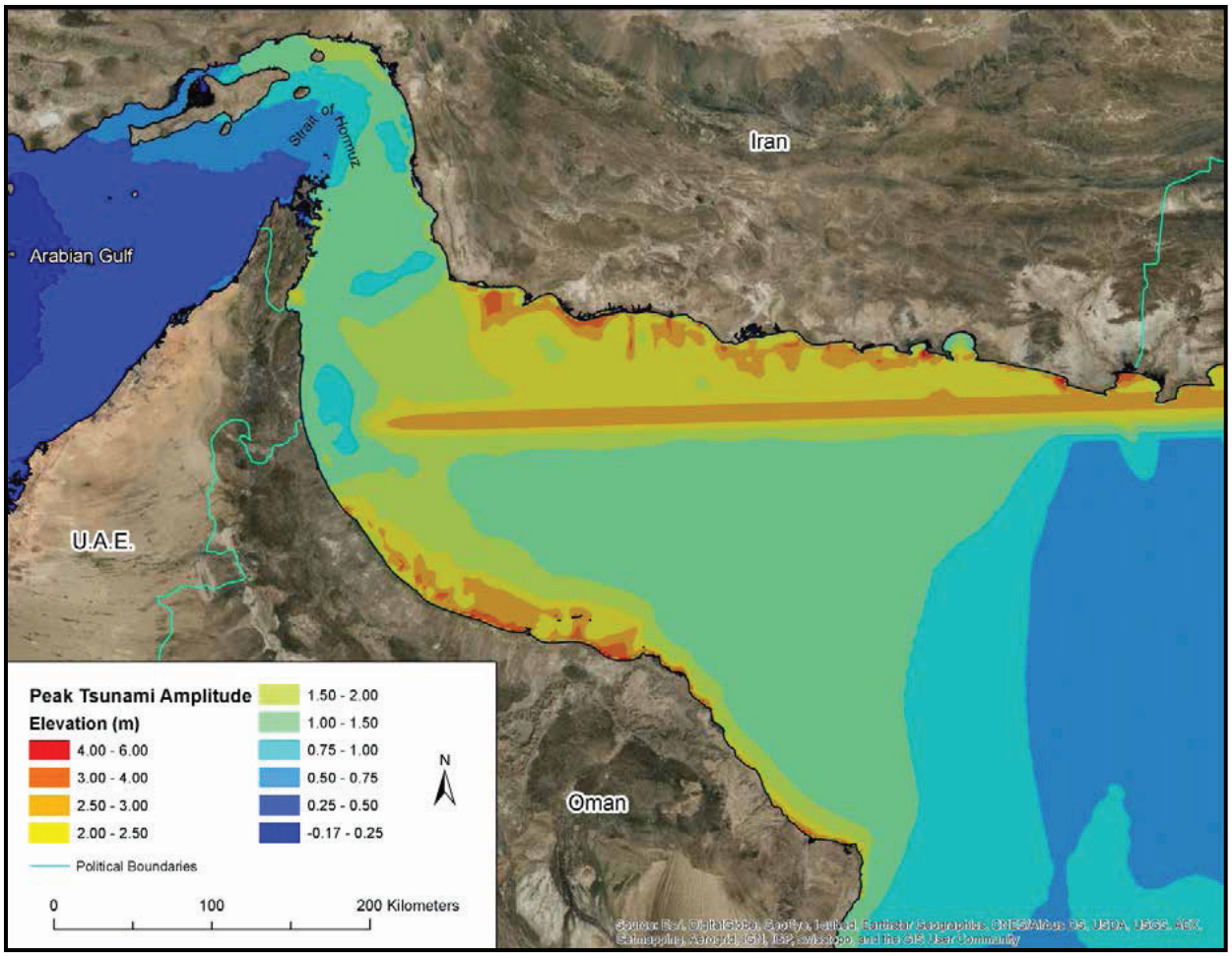

Figure 7: Peak Tsunami Wave Amplitudes for M_w 9.0 Earthquake Event – Western Arabian Sea

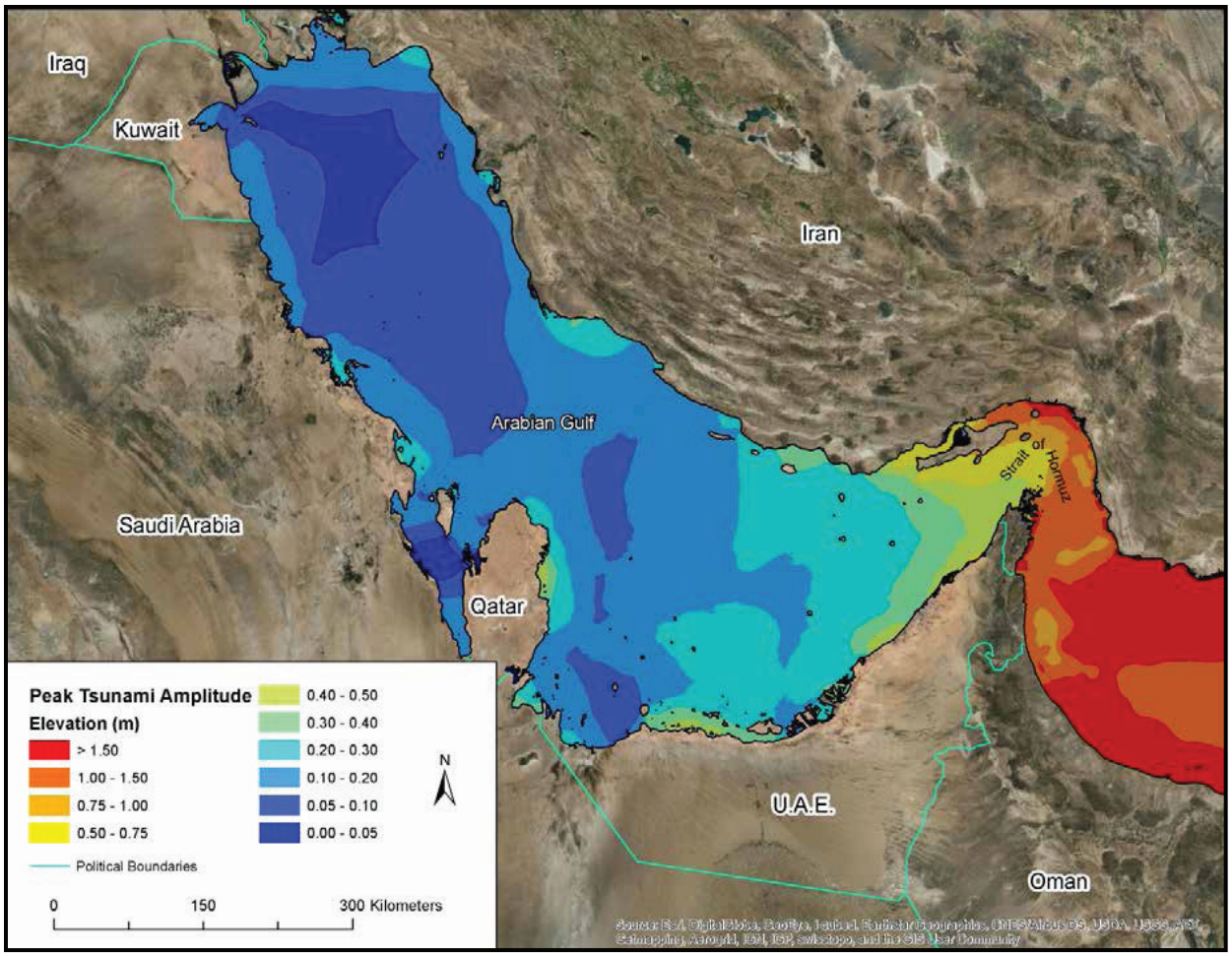

Figure 8: Peak Tsunami Wave Amplitudes for M_w 9.0 Earthquake Event – Arabian Gulf

CONCLUSIONS

This study evaluated the potential for a tsunami originating in the Makran Subduction Zone (southern coast of Iran and Pakistan in the Arabian Sea) to impact the shorelines of the western Arabian Sea and the Arabian Gulf. The Makran Subduction Zone geometry was evaluated to develop a conservative earthquake scenario. The associated sea floor displacement was computed and used as input to a tsunami propagation model. The tsunami model was calibrated to the tsunami caused by the great 1945 Makran earthquake.

The results indicate that rupture along the entire length of the Makran Subduction Zone (approximately a M_w 9.0 earthquake event) would initiate large tsunami waves (up to 6 meters in some locations) along the shorelines of the western Arabian Sea. However, even with full rupture of the MSZ, minimal tsunami impact is expected inside the Arabian Gulf. Peak tsunami wave amplitudes on the shorelines of the Arabian Gulf were computed to range from about 0.05 meters to 0.5 meters in different locations.

REFERENCES

Bilham, R., Lodi; S., Hough, S.; Bukhary, S.; Murtaza, K. A.; and Rafeeqi, S. F. A. (2007). "Seismic hazard in Karachi, Pakistan: uncertain past, uncertain future," *Seismological Research Letters*, 78(6), 601-613.

Byrne, D. E.; Sykes, L. R.; and Davis, D. M. (1992). "Great thrust earthquakes and aseismic slip along the plate boundary of the Makran subduction zone," *Journal of Geophysical Research*, 97(B1), 449-478.

Deltares (2011). "Delft3D-FLOW: Simulations of multi-dimensional hydrodynamic flows and transport phenomena, including sediments," User Manual, Version 3.15.

Heidarzadeh, M.; Pirooz, M. D.; Zaker, N. H.; Yalciner, A. C.; Mokhtari, M.; Esmaeily, A. (2008). "Historical tsunami in the Makran subduction zone off the southern coasts of Iran and Pakistan and results of numerical modeling," *Ocean Engineering*, 35, 774-786.

Heidarzadeh, M.; Pirooz, M. D.; Zaker, N. H.; and Yalciner, A. C. (2009). "Preliminary estimation of the tsunami hazards associated with the Makran subduction zone at the northwestern Indian Ocean," *Natural Hazards*, 48, 229-243.

Okada, Y. (1985). "Surface deformation due to shear and tensile faults in a half-space," *Bulletin of the Seismological Society of America*, 75(4), 1135-1154.

Okal, E. A. and Synolakis, C. E. (2008). "Far-field tsunami hazard from mega-thrust earthquakes in the Indian Ocean," *Geophysical Journal International*, 172, 995-1015.

Rajendran, C. P.; Ramanamurthy, M. V.; Reddy, N. T.; and Rajendran, K. (2008). "Hazard Implications of the Late Arrival of the 1945 Makran Tsunami," *Current Science*, 95(12), 1739-1743.

Strasser, F. O.; Arango, M. C.; and Bommer, J. J. (2010). "Scaling of the source dimensions of interface and intraslab subduction-zone earthquakes with moment magnitude," *Seismological Research Letters*, 81(6), 941-950.

Synolakis, C.; Liu, P.; Carrier, G.; and Yeh, H. (1997). "Tsunamigenic sea-floor deformations," *Science*, 278, 598-600.

Ward, S. (1989). "Tsunamis," *Encyclopedia of Physical Science and Technology*, Academic Press, 17, 175-191.